Available online at www.sciencedirect.com
ScienceDirect
Trans. Nonferrous Met. Soc. China 32(2022) 1205−1216
Transactions of Nonferrous Metals Society of China
www.tnmsc.cn

Evolution of Goss texture in thin-walled copper tube at different heat treatment temperatures

Song-wei WANG[1], Hong-wu SONG[1], Yan CHEN[1], Qi YU[1,2], Shi-hong ZHANG[1]

1. Shi-changxu Innovation Center for Advanced Materials, Institute of Metal Research, Chinese Academy of Sciences, Shenyang 110016, China;
2. Jiangxi Copper Corporation Co., Ltd., Nanchang 330096, China

Received 31 March 2021; accepted 8 December 2021

Abstract: The evolution of microstructure, textures, and mechanical properties of thin-walled copper tube during heat treatment was investigated using EBSD technique and tensile test. The results show that the initial deformation textures of pre-drawn thin-walled copper tube are mainly composed of Copper and Y components, while with the increase of temperatures, the textures are transformed into a strong Goss texture gradually. The high-resolution microstructural characterizations indicate that the new Goss recrystallized grains nucleate and grow up within the deformed Copper grains and Y grains in different mechanisms, respectively. The tensile strength of the thin-walled copper tube decreases gradually with the increase of the temperature, while the elongation increases first and then decreases sharply due to the action of grain sizes and texture components.

Key words: thin-walled copper tube; recrystallization behavior; Goss texture; nucleation mechanism; annealing twin

1 Introduction

The thin-walled copper tube is the key component to fabricate miniature heat pipe, which is widely used to dissipate high heat fluxes in the electronic devices [1,2]. The copper tube has been pre-drawn firstly to obtain a certain strength, and then operated at an elevate temperature (>900 °C) according to the process requirements of heat pipes. In our previous work, the relationship between microstructural parameters and the surface roughening problem was investigated, and it was found that the surface roughness can be influenced both by grain size and texture components of copper tube [3]. Generally, the pure copper tube has a lower recrystallization temperature around 200 °C [4], while microstructure and texture at a high temperature are still lack of investigation. Especially for the requirements of good formability and surface quality of the annealed tubes, it is necessary to better understand the recrystallization process and grain growth during the heat treatment.

The recrystallization behavior of pure copper is quite different due to the conditions of pre-deformation. Researchers have investigated the recrystallization of various grades of copper by using both in situ and post facto analyses [5,6]. Cold drawn copper wire with a 38% reduction was observed to recrystallize above 200 °C [7], other studies have reported the initiation of recrystallization at 210 °C [8]. BAUDIN et al [5] proposed that the ⟨100⟩ fiber increases at the expense of the other texture components after recrystallization. The effect of cold rolling process on texture evolution of pure copper has been well investigated [9−12], and the results reveal that the Cube orientation is the main recrystallization texture and the formation mechanisms have been proposed as the oriented growth theory. ANAND

Corresponding author: Yan CHEN, Tel: +86-15004050792, E-mail: ychen10b@imr.ac.cn
DOI: 10.1016/S1003-6326(22)65867-9

et al [13] characterized the annealed pure copper sheet after cryo-rolling process and found that the sample shows a weakening of Brass texture with the increase of annealing time, then exhibits almost random texture and finally forms the strong Cube texture. While the cold rolled Al−0.3%Cu develops a strong Goss texture during annealing treatment which is related to the oriented nucleation mechanism [14]. LEE [15] proposed the strain energy release maximization model to predict the texture evolution of copper electrodeposits after recrystallization. Also, HAMDANY et al [16] used the synchrotron diffraction method to investigate the local texture gradient through the wall thickness of SF-Cu tubes with an average wall thickness of 10 mm. The structure consists of recrystallized equiaxed grains with twins and the dominant texture component is the {001}⟨100⟩ Cube component.

In summary, the origin of recrystallization textures is usually explained through oriented nucleation or oriented growth [17]. In the oriented nucleation hypothesis, grains with a particular orientation prefer to nucleate and determine the final recrystallization texture; on the other hand, oriented growth indicates that only grains with the best orientation related to the deformed matrix can grow and form the recrystallization texture. Additionally, annealing twins are an important microstructural feature of pure copper with a medium stacking fault energy (SFE). The recrystallization twinning may: (1) lead to new orientations that do not exist in the original deformation texture, and/or (2) contribute to the nucleation during the early stages of recrystallization [18].

The aim of the present investigation is to clarify the origin, evolution of grain orientations and their statistical appearance in the textures of thin-walled copper tube treated at the elevate temperatures. The results also outline the trend of mechanical properties during heat treatment. The study on the development of recrystallization textures considered the unique initial deformation texture produced by tube drawing process [19], which is of great scientific and technological importance.

2 Experimental

The material used in this research was the highly purified copper (>99.99%, mass fraction) in the form of thin-walled tubes, with a size of 6 mm in diameter and 0.3 mm in thickness. The tubes were obtained by the float-plug drawing process with the area reduction of about 30%. To examine the microstructure and texture evolution during sintering treatment, the tubes were heated in the box-type resistance furnace from room temperature to 900 °C with the heating rate as follows: 1 °C/s for the section below 500 °C, 0.2 °C/s for the section of 500−700 °C and 0.1 °C/s for the section of 700−900 °C. Prior to the heat treatment, the tube samples were vacuum encapsulated in a quartz tube to prevent oxidation of surface. The tube samples were taken out one by one when the temperature reached 300, 500, 700 and 900 °C, respectively, and then water quenched immediately to maintain the microstructure.

The microstructures of the as-drawn and annealed tubes were evaluated by using electron backscattered diffraction (EBSD) technique. The samples with a size of 5 mm in length (drawing direction, DD), 3 mm in width (circumferential direction, CD) and 0.3 mm in thickness (radial direction, RD) were cut from the tube walls, as seen in Fig. 1. The DD−CD plane served as an observation surface was ground slightly to obtain a smooth plane, and then polished with diamond paste and finished with ion milling to remove the surface deformation layer. The EBSD tests were carried out using an FEI Nova Nano SEM 430 field-emission scanning electron microscope equipped with a fully automatic HKL Technology EBSD attachment operated at 20 kV. The evaluation of microstructure and the fractions of texture components were characterized by Channel 5 software applying a 5° deviation from the closest exact {*hkl*}⟨*uvw*⟩ orientation. The orientation distribution function (ODF) accordingly was calculated using the Atex software. The tensile tests were carried out using an Instron−8801 testing machine with the maximum load of 10 kN at room temperature and the strain rate of $3\times10^{-3}\ s^{-1}$. The whole tube billets (*d*6 mm × 0.3 mm) were used as the specimens, the length of the gauge section was 200 mm and both ends of the tube were flattened to facilitate clamping.

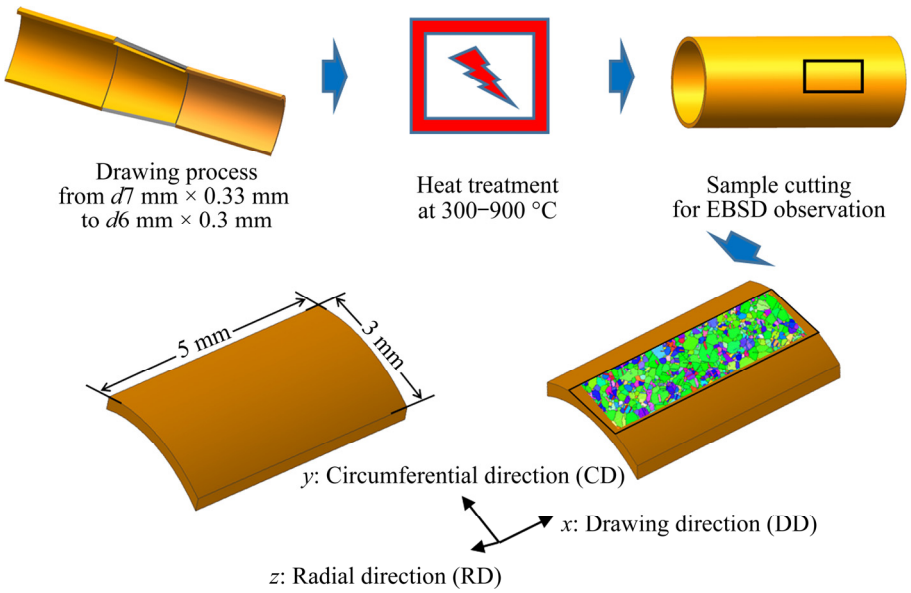

Fig. 1 Schematic of processing and observation surface of samples for EBSD measurement

3 Results and discussion

3.1 Microstructure and texture evolution during annealing

Figure 2 shows the microstructure and deformation texture of the initial copper tube (as-drawn). The misorientation angles with $2°\leq\theta<15°$ and $\theta\geq15°$ are referred as low angle grain boundaries (LAGBs) and high angle grain boundaries (HAGBs), which were marked with gray line and black line, respectively. The microstructure of the as-drawn copper tube clearly shows that the grains were elongated along the drawing direction (Fig. 2(a)) with a large number of LAGBs within them. The initial as-drawn tube mainly consists of three different texture components, as shown in Fig. 2(b), a quite pronounced Copper component in dominate (43.9%), some Y component (22.7%), and a small Goss component (12.5%). Previous studies have reported the texture evolution of copper tube and its relationship with the strain during the float-plug drawing process [19].

Figure 3 shows the evolution of the microstructure and textures with increasing the annealing temperature. The textures of the copper tube at different heating stages reveal significant differences both quantitatively and qualitatively. It is obvious that the initial Copper component and Y component weaken with the increase of temperature; on the other hand, the Goss component increases continuously and becomes the dominant component. Figure 4 summarizes the microstructure parameters from the EBSD maps, e.g. grain size and the grain boundary characters, for as-drawn tube and subsequently annealed samples. At 300 °C of heat treatment in Figs. 3(a_1, a_2), the area fraction of Goss component increases slightly; however, the microstructure remains the deformed state as dominant due to the shortage of holding time. A transformation from elongated grains to the equiaxed ones may start at this temperature on account of the new grains generated in the local regions of deformed bands. The recrystallization process and subsequent grain growth were manifested in terms of a sharp increase of grain size and reduction in the fraction of LAGBs as seen in Fig. 4. The pure copper has a medium SFE equal to 78 mJ/m^2 [17]. As is known to all, the stored energy in deformation is the driving force for recovery and recrystallization phenomena. The extent of recovery is governed by SFE. The pure copper with medium SFE, in which cross slip and climb dislocation are difficult to be activated, shows little recovery prior to recrystallization [20]. As a result, the fraction of LAGBs changes little before 300 °C, as seen in Fig. 4(b). When the temperature arises, the grains with Goss orientation have an advantage in size over other grains, leading to the dominant texture of

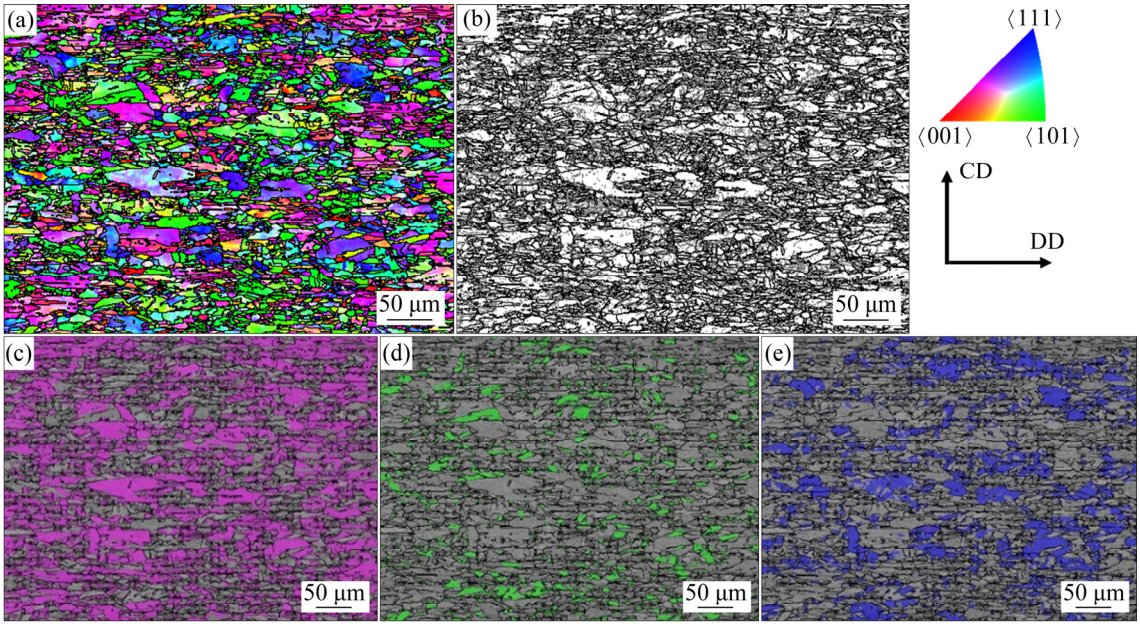

Fig. 2 Microstructure and texture components of initial (as-drawn) copper tube: (a) IPF map; (b) Distribution of LAGBs; (c) Copper component; (d) Goss component; (e) Y component

annealed copper tube, as seen in Figs. 3(c_1, c_2) and (d_1, d_2). And then these Goss-grains encounter each other and form LAGBs, resulting in a slight increase of LAGBs and a reduction of HAGBs after 500 °C as shown in Fig. 4(b).

It is important to notice that the twin relationship boundaries marked as Σ3 boundaries increase in the annealed tube, which shows a similar trend of HAGBs (seen in Fig. 4(b)). It is commonly known that the annealing twin formation is related to the "growth accident", namely, the coherent twin boundaries are generated at migrating grain boundaries due to the occurrence of stacking errors [21]. In general, the interfacial energy of the twin boundary is fairly low due to the coherent feature. The previous research indicated that for the FCC metals with low or medium SFE, annealing twinning is the only process that creates new orientations during recrystallization [18,22,23]. The evolution of annealing twins in the copper tube during recrystallization has been discussed in the previous report [24].

In order to examine the texture evolution in a statistically significant way, the orientation distribution function (ODF) has been computed from the EBSD data. Figure 5 represents φ_2=45° section of the ODF for the as-drawn and annealed tube samples. Figure 5(a) reveals the presence of strong Copper component, minor Y component and weak Goss component in the as-drawn tube. During the annealing treatment, there is a significant drop of Copper component and a gradual decrease of Y component; on the contrary, the Goss component increases obviously. The overall texture intensity also increases significantly with the increase of temperature. It is noticed that a low fraction of Cube component appears at the early stage of the recrystallization; however, the Cube component cannot compete with the Goss component during the grain growth stage and disappears gradually.

3.2 Formation and growth of Goss-oriented grains during recrystallization

It is clearly observed from the microstructure at 300 °C that the recrystallization process already takes place in the elongated grains of as-drawn state. A large number of recrystallized grains with Goss orientation begin to nucleate, but the proportion of overall Goss texture does not increase much, mainly because the new nucleated grains have not yet begun to grow. To investigate the formation of the new grains, the local analysis was performed by EBSD observation. Figure 6 shows the static recrystallization (SRX) behavior in the deformed grains at the local position of Fig. 3(a_1) (marked in white rectangle). The HAGBs and LAGBs are

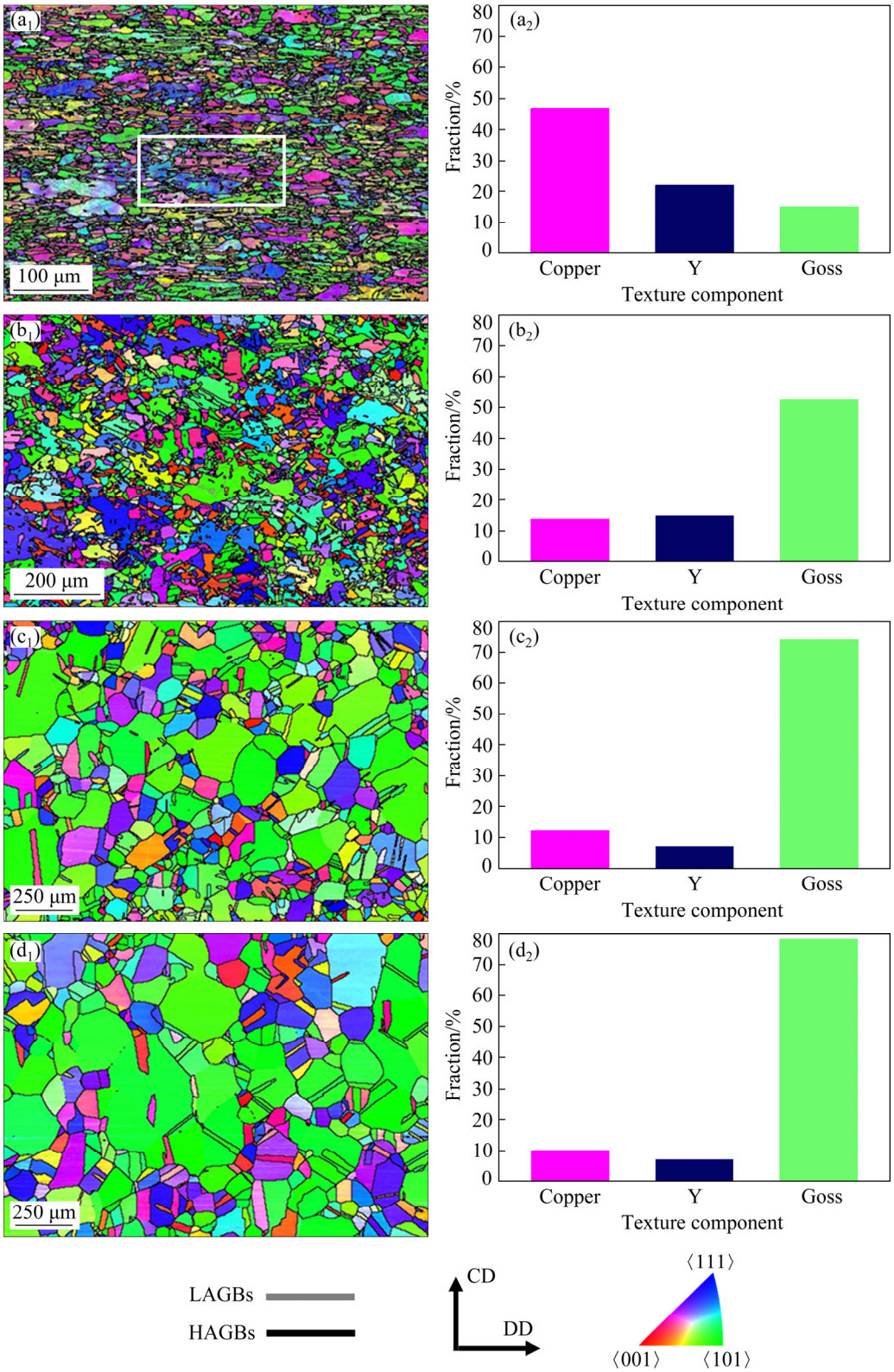

Fig. 3 Microstructures and texture components of copper tube annealed at different temperatures: (a_1, a_2) 300 °C; (b_1, b_2) 500 °C; (c_1, c_2) 700 °C; (d_1, d_2) 900 °C

marked in black lines and white lines, respectively. Figure 6(a) indicates some fine SRX grains with Goss orientation (marked in white dotted circle) are generated both along the deformed grain boundaries and within the grains. Obviously, these new Goss grains appear both in parent grains with Copper orientation and Y orientation. Thus, the increase of Goss grains is at the expense of Copper and Y

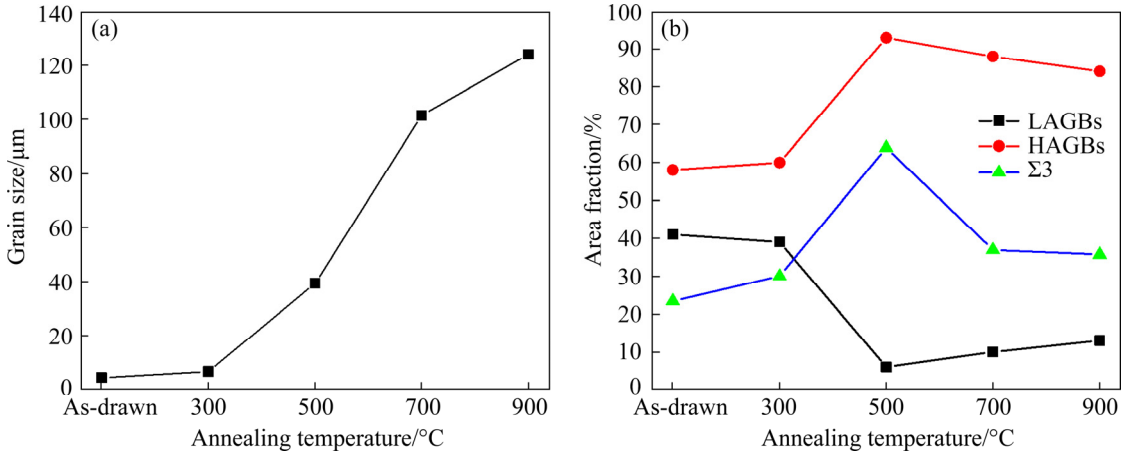

Fig. 4 Variation of grain size (a) and grain boundary characters (b) during annealing treatment

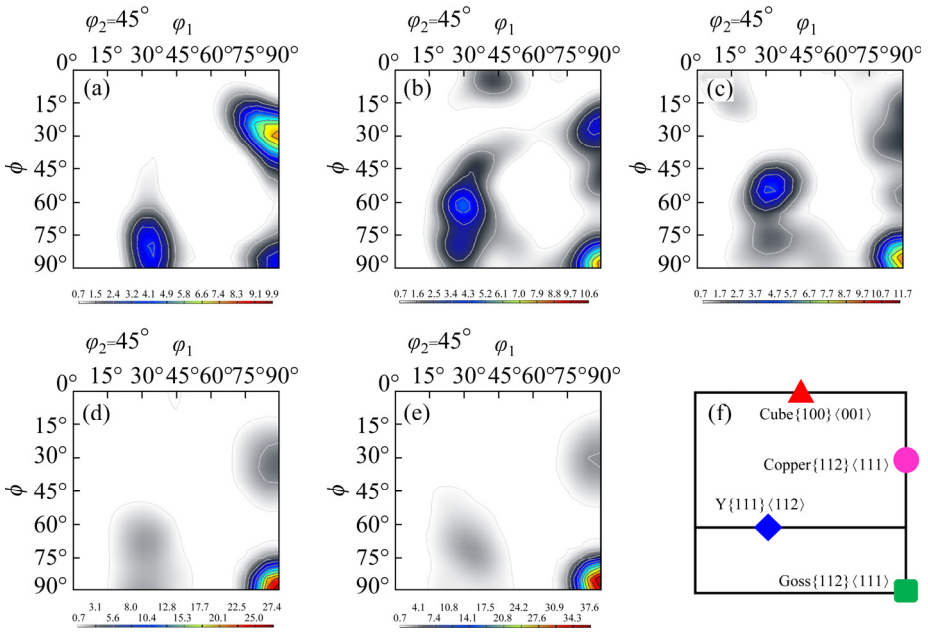

Fig. 5 Orientation distribution function maps with φ_2=45° section for as-drawn (a), annealed at 300 °C (b), 500 °C (c), 700 °C (d) and 900 °C (e) tube samples, and ideal texture component (f)

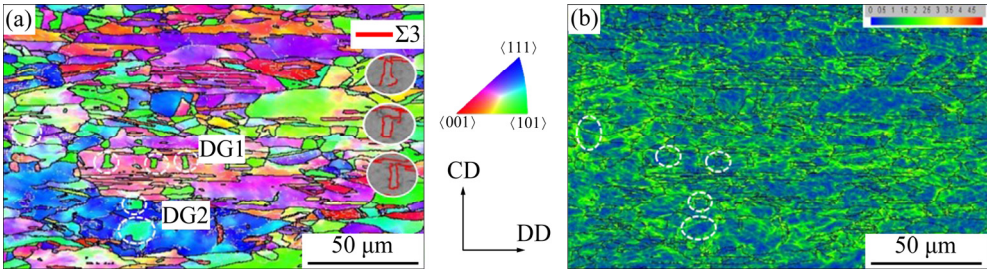

Fig. 6 SRX behavior in deformed grains at 300 °C: (a) Recrystallized grains with Goss orientation formed along deformed grains; (b) KAM map showing stored energy distribution

components, which is in accordance with the change of texture components. The KAM (kernel averaged misorientation) map shown in Fig. 6(b) reveals the KAM value of regions with new Goss grains is relatively low. These new grains are produced on the base of releasing the degree of plastic strain induced by former deformation, which was assessed by local misorientation in

Fig. 6(b) [25]. It is believed that the static recrystallization is induced by the high concentration of defects (primary vacancies) in the deformed materials, which significantly enhance grain boundary mobility and serve as the driving force for boundary migration [26]. The origin of recrystallization in the copper has been proved to be related to grain boundary bulging [27]. The growth of new grains can be judged by evaluating the grain boundaries. The side of grains having a flat and curved shape boundary is usually the probable starting point of recrystallized nuclei on the high angle boundary, while the other side of grains shows different grain boundary bulges at the front of recrystallized grain boundary. The new grains within DG1 (DG represents deformed grain) can be judged to nucleate along the straight boundary of deformed grain. Other new grains can be seen to be surrounded by heavily deformed grains which include a low dislocation/defect density and are divided into some subgrains, as seen in DG2. Figure 6(b) shows that there are low misorientations between different areas with straight boundaries which are probably polygonised into finer subgrains with arrangement of dislocations inside the grain.

To analyze the orientation transformation, the deformed grains can be divided into two types: (1) Copper orientation such as DG1 and (2) Y orientation such as DG2. The two types of grains endured the large deformation, that is why a high aspect ratio formed in shape, as seen in Fig. 2(b).

Figure 7 shows the SRX behavior of the Copper-oriented DG1. In DG1, several new grains possessing twin boundary relationship with parent grain were observed (as seen from white circles marked in Fig. 6). These new recrystallized grains (RGs) nucleated near the original boundaries of deformed grain, and then grew up in terms of annealing twins. Figure 7(a) shows the three-dimensional (3D) crystallographic relationship between recrystallized grain and the parent grain, as well as the corresponding Euler angles. With the Euler angles, it is calculated that the misorientation angle between the recrystallized grain (RG1) and the deformed grain (DG1) is confirmed to be 55.6° [$\bar{1}\bar{1}$1] relationship. Figure 7(b) shows the orientation of the RG1 with respect to DG1, corresponding to {111} pole figure. Figure 7(c) shows the line profile of the misorientation angle along with Arrow AB in Fig. 6(a). The line profile

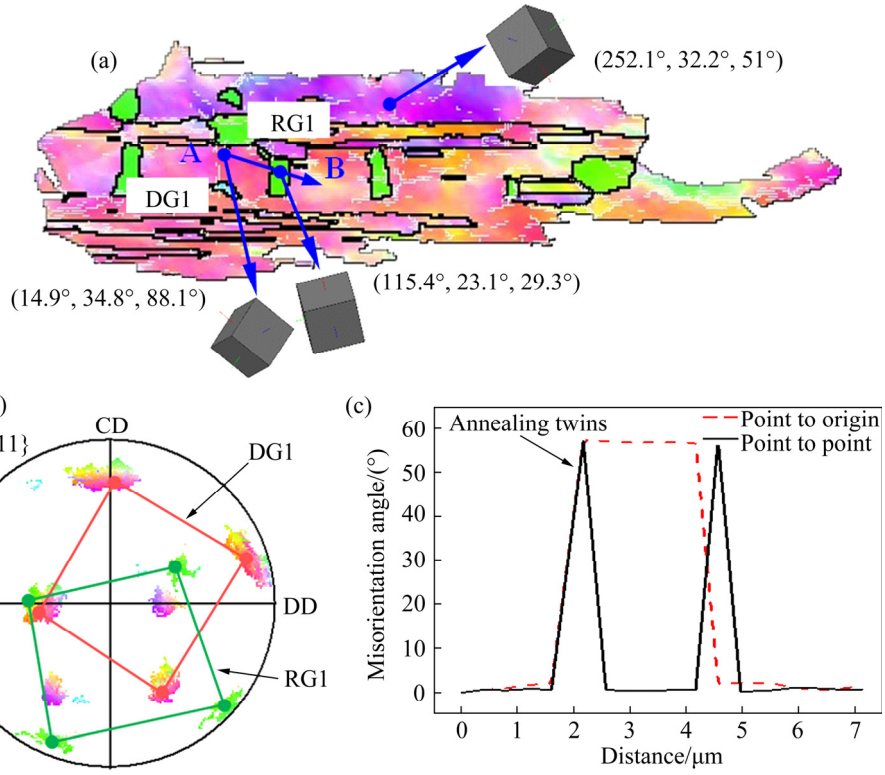

Fig. 7 SRX behavior of DG1 with Copper orientation selected in Fig. 6(a): (a) 3D crystal cube with Eular angles; (b) Corresponding crystallographic orientations in {111} pole figure; (c) Line profile of misorientation angle along Arrow AB in (a)

of point-to-origin indicates the distinct discontinuity of orientations at the twin boundaries of the new grains, while the misorientation of point-to-point result indicates almost no change within RG1. The formation of these strain-free grains within a cold-worked material usually occurs with the annealing process. In present research, the recrystallized grains show the twinning relationship with parent grain, as depicted by the 3D crystal cube along Arrow AB, which is very close to the ideal Goss orientation. This result has been confirmed by previous research. Some hypotheses were proposed in order to explain annealing twin produced at the beginning of the recrystallization [28−30], which is based on GB energy, mobility, and reorientation, respectively. Regarding these principles, annealing twin is only controlled by the decrease in interfacial energy due to the orientation change.

Figure 8 shows the SRX behavior within the DG2. It is clear to see the green region (RG2) and a small part of red one (RG3) produced within the blue parent DG2. Figure 8(a) also presents the 3D crystal cube to better understand the relationship of each part, and the Euler angles are also provided to accurately calculate the crystal orientations. The corresponding crystallographic orientations are presented in {111} pole figure in order to interpret their relationships, as shown in Fig. 8(b). From the Euler angles calculation results, the green region (RG2) shows a 12.6° deviation to the ideal Goss orientation, which conforms to the error range of 15°. The red grain has a Cube orientation with respect to the parent grain. The line profile of point-to-origin along the red arrow CD shows that the misorientation angle increases gradually up to 15° from the blue region to green region, as seen in Fig. 8(c), indicating the continuous change of orientation occurring in DG2. While the point-to-point misorientation within the green region shows a relatively low value compared to that within the blue region, that is to say, the green region is the origin of the recrystallized grain. It can be determined that the orientations of two regions were close, while the blue region clustered around the Y component and the green region tended to be Goss component. The result suggests the gradual transformation of texture from Y to Goss. This can be further confirmed by the 3D crystal cubes along the CD direction. Thus, the green region will continue to grow at the expense of the parent grains. The new grains with Cube orientation may be swallowed by the Goss grains due to their growth advantage.

At the beginning of the recrystallization, the new grains are favorable to form in a near Goss

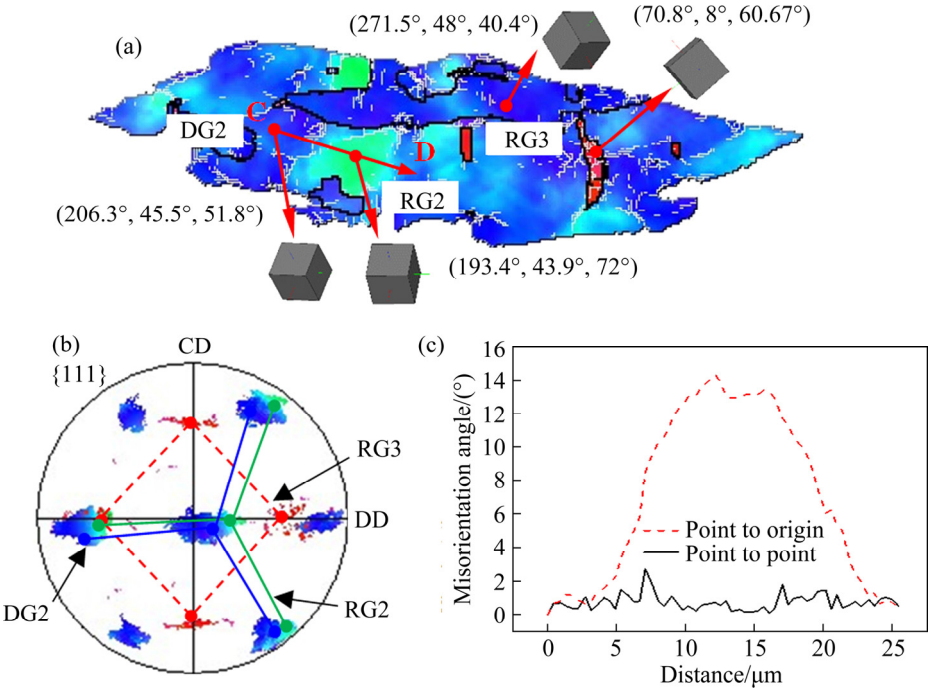

Fig. 8 SRX behavior of DG2 with Copper orientation selected in Fig. 6(a): (a) 3D crystal cube with Eular angles; (b) Corresponding crystallographic orientations in {111} pole figure; (c) Line profile of misorientation angle along Arrow CD in (a)

relationship with the deformed structure. Two types of Goss-oriented regions were discovered in deformed grains with {112}⟨111⟩ (Copper) orientation and {111}⟨112⟩ (Y) orientation, respectively. Previous researchers have described that after cold rolling, Goss orientations evolved within the shear bands in the {111}⟨112⟩ and {111}⟨110⟩ deformed grains [31,32]. The preferential nucleation of Goss grains is considered to be related to its low stored energy [33−36]. The KAM map (Fig. 6(b)) also indicates that the Goss-oriented regions contain a much lower dislocation density than the regions of the Copper and Y components. Thus, there is a driving force for lower-energy Goss grains to grow up in the deformed matrix with a higher stored energy. Moreover, the 60°⟨111⟩ relationship between the Goss grains and deformed grains has a higher migration rate. Thus, with the increase of temperature, the Goss grains grow up rapidly at the expense of the surrounding deformed grains. The rapid growth of grains results in the formation of the strong Goss texture in the copper tube. It is noticed that some Cube-oriented regions are formed in the deformed Y grains. The origin of Cube recrystallization texture in the pre-rolled copper is well established. The possession of a near Σ7 misorientation between the new cube grains and a major component of the deformation texture S {123}⟨634⟩ is responsible for the perfect Cube texture after annealing. But in the present result, the Cube texture at the early stage of recrystallization is just in a small fraction, which cannot compete with the Goss texture as seen in Fig. 5. That is to say, the recrystallization texture is quite different from the deformation texture.

3.3 Evolution of mechanical properties

Figure 9(a) shows the engineering stress−engineering strain curves for the as-drawn tube and annealed tubes. Figure 9(b) shows the ultimate tensile strength (UTS) and elongation extracted from the curve varying with the area fraction of the Goss component. It is already known that the Goss component grows rapidly with the increasing temperature. Figure 9(b) shows that the UTS decreases gradually with the increase of Goss content, while the ductility increases first and then decreases. Two reasons may account for the continuous decline in tensile strength. (1) At the early stage of annealing treatment, the softening performance was induced by the recovery which involved the redistribution and annihilation of dense dislocations without the formation of boundaries. Therefore, although the grain size did not change significantly in the initial stage (Fig. 4(a)), the tensile strength of the copper tube decreased obviously, and the elongation increased. (2) In the recrystallization and grain growth period, the decrease of tensile strength was mainly related to the variation of grain size (Fig. 4(a)), like the well-known Hall−Petch relation [37,38]. It is interesting that the elongation of the tube reaches the maximum value of about 36% at the point of Goss fraction near 50%, and then decreases sharply with the continuous increase of Goss fraction. The deformation ability of the grains with different orientations was considered by comparing the Schmid factor under uniaxial load, as shown in Fig. 10. The Goss grains show the highest Schmid factor value, followed by the Copper grains, and the Y grains have the lowest value. That is to say, the Goss grains are the “soft” oriented components and

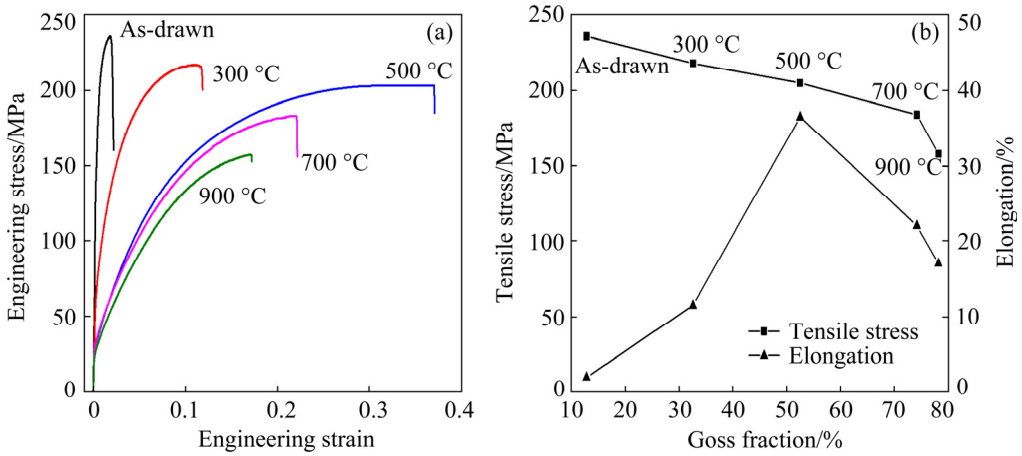

Fig. 9 Engineering stress−engineering strain curves at each state (a), and tensile stress and elongation (b) of copper tube samples

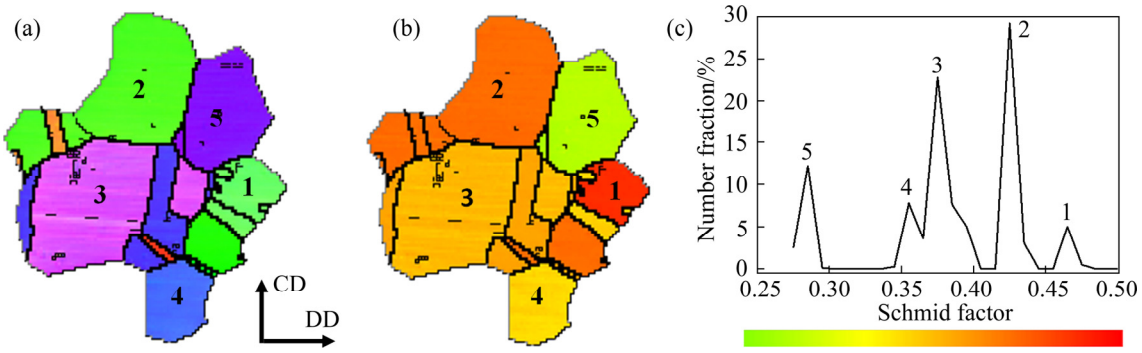

Fig. 10 Selection of local grains with different orientations and comparison of Schmid factor values under uniaxial tensile test along DD: (a) IPF of grains selected from Fig. 3(c); (b) Distribution of Schmid factor in grains; (c) Comparison of Schmid factor values (1−5 in Fig. 10 represent the number of the selected grains)

can present better plasticity than the other two components which are the "hard" oriented components. Although the tensile deformation behavior is complicated with such a high elongation, we can also consider that the increase of Goss orientations may contribute to good plasticity of copper tube. However, the elongation curve meets an inflection point at 500 °C and then begins to decline. At this temperature point, the average grain size begins to increase at a greater rate and the Goss texture composition exceeds 50%, which indicates that heavy growth of the Goss-oriented grains causes a serious decrease in plasticity.

4 Conclusions

(1) The texture components of thin-walled copper tubes change significantly, from the initial Copper and Y components to Goss component, during high temperature heat treatment. A slight fraction of Cube component was produced at the early stage of the recrystallization, and then disappeared gradually during the grain growth stage.

(2) The origin of Goss recrystallized grains during recrystallization process has been proved in two kinds of mechanisms: nucleating near the original boundaries of deformed grain, then growing up in terms of annealing twins; nucleating within the deformed grains which are probably polygonised into finer subgrains with arrangement of dislocations inside the grain.

(3) The tensile strength of the thin-walled copper tube decreases gradually during the annealing temperature, while the elongation reaches the peak value of about 36% at 500 °C and then decreases sharply.

Acknowledgments

This work was financially supported by the China Postdoctoral Science Foundation (No. 2019M662276) and the Chinese Academy of Science and Technology Service Network Planning (No. KFJ-STS-QYZD-145).

References

[1] ZEGHARI K, LOUAHLIA H. Flat miniature heat pipe with sintered porous wick structure: Experimental and mathematical studies [J]. International Journal of Heat and Mass Transfer, 2020, 158: 120021.

[2] JOUHARA H, CHAUHAN A, NANNOU T, ALMAHMOUD S, DELPECH B, WROBEL L C. Heat pipe based systems—Advances and applications [J]. Energy, 2017, 128: 729−754.

[3] WANG S W, ZHANG S H, SONG H W, CHEN Y. Surface roughness improvement of the bent thin-walled copper tube by controlling the microstructure and texture components [J]. Procedia Manufacturing, 2020, 50: 613−617.

[4] TAYLOR S, MASTERS I, LI Z, KOTADIA H R. Influence of elevated temperatures on mechanical properties and microstructure of C106 copper investigated by in situ heated stage EBSD analysis [J]. Metallurgical and Materials Transactions A, 2019, 50(10): 4493−4497.

[5] BAUDIN T, ETTER A L, PENELLE R. Annealing twin formation and recrystallization study of cold-drawn copper wires from EBSD measurements [J]. Materials Characterization, 2007, 58(10): 947−952.

[6] FIELD D, BRADFORD L, NOWELL M, LILLO T. The role of annealing twins during recrystallization of Cu [J]. Acta Materialia, 2007, 55(12): 4233−4241.

[7] BRISSET F, HELBERT A L, BAUDIN T. In situ electron backscatter diffraction investigation of recrystallization in a

copper wire [J]. Microscopy and Microanalysis, 2013, 19(4): 969−977.
[8] SCHWARJZ A J, KUMAR M, ADAMS B L, FIELD D P. Electron backscatter diffraction in materials science [M]. 2nd ed. Boston: Springer, 2009.
[9] SUWAS S, RAY R K. Crystallographic texture of materials [M]. London: Springer, 2014.
[10] GU C F, TOTH L S, ZHANG Y D, HOFFMAN M. Unexpected brass-type texture in rolling of ultrafine-grained copper [J]. Scripta Materialia, 2014, 92: 51−54.
[11] SIDOR J J, KESTENS L A I. Analytical description of rolling textures in face-centred-cubic metals [J]. Scripta Materialia, 2013, 68(5): 273−276.
[12] MAO Z N, GU R C, LIU F, LIU Y, LIAO X Z, WANG J T. Effect of equal channel angular pressing on the thermal-annealing-induced microstructure and texture evolution of cold-rolled copper [J]. Materials Science and Engineering A, 2016, 674: 186−192.
[13] ANAND G, BARAI K, MADHAVAN R, CHATTOPADHYAY P P. Evolution of annealing texture in cryo-rolled copper [J]. Materials Science and Engineering A, 2015, 638: 114−120.
[14] SHUAI L F, HUANG T L, WU G L, HUANG X, MISHIN O V. Development of Goss texture in Al−0.3%Cu annealed after heavy rolling [J]. Journal of Alloys and Compounds, 2018, 749: 399−405.
[15] LEE D N. Strain energy release maximization model for recrystallization textures [J]. Metals and Materials, 1999, 5(5): 401−417.
[16] AL-HAMDANY N A, BROKMEIER H G, SALIH M, ZHONG Z Y, SCHWEBKE B, SCHELL N, GAN W. Crystallographic texture gradient along the wall thickness of an SF-copper tube [J]. Materials Characterization, 2018, 139: 125−133.
[17] HUMPHREYS F J, HATHERLY M. Recrystallisation and related annealing phenomena [M]. 2nd ed. Oxford: Elsevier, 2004.
[18] GOTTSTEIN G. Annealing texture development by multiple twinning in FCC crystals [J]. Acta Metallurgica, 1984, 32(7): 1117−1138.
[19] WANG S W, CHEN Y, SONG H W, EL-ELATY A A, LIU J S, ZHANG S H. Investigation of texture transformation paths in copper tube during floating plug drawing process [J]. International Journal of Material Forming, 2021, 14(4): 563−575.
[20] ROOHOLLAH J. Unexpected cube texture in cold rolling of copper [J]. Materials Letters, 2017, 202: 111−115.
[21] MAHAJAN S. Critique of mechanisms of formation of deformation, annealing and growth twins: Face centered cubic metals and alloys [J]. Scripta Materialia, 2013, 68(2): 95−99.
[22] HAASEN P, WILBRANDT P J. Formation of the recrystallization texture in deformed single crystals [J]. Materials Science Forum, 1994, 157: 887−898.
[23] BACROIX B, DRIVER J H, GALL R L, MAURICE C, PENELLE R, REGLE H, TABOUROT L. Nucleation in recrystallization [J]. Materials Science Forum, 2004, 467: 107−116.
[24] WANG S W, SONG H W, CHEN Y, ZHANG S H, LI H H. Evolution of annealing twins and recrystallization texture in thin-walled copper tube during heat treatment [J]. Acta Metallurgica Sinica (English Letters), 2020, 33: 1618−1626.
[25] MASAYUKI K. A smoothing filter for misorientation mapping obtained by EBSD [J]. Materials Transactions, 2010, 51(9): 1516−1520.
[26] KONKOVA T, MIRONOV S, KORZNIKOV A, SEMIATIN S L. Microstructural response of pure copper to cryogenic rolling [J]. Acta Materialia, 2010, 58(16): 5262−5273.
[27] AGHAMIRI S M S, ZHANG S H, UKAI S, OONO N, KASADA R, NOTO H, HISHINUMA Y, MUROGA T. Microstructure development in cryogenically rolled oxide dispersion strengthened copper [J]. Materialia, 2020, 9: 100520.
[28] SCHULZ U, WILBRANDT P J, TIDECKS R. Growth and crystallographic orientations of zinc and zinc−silver whiskers [J]. Journal of Crystal Growth, 1987, 85(3): 472−476.
[29] ZHANG P C, SHI J F, YU Y S, SUN J C, LI T J. Effect of cryorolling on microstructure and property of high strength and high conductivity Cu−0.5wt.%Cr alloy [J]. Transactions of Nonferrous Metals Society of China, 2020, 30(9): 2472−2479.
[30] FORM W, GINDRAUX G, MLYNCAR V. Density of annealing twins [J]. Metal Science, 1980, 14(1): 16−20.
[31] HARATANI T R, HUTCHINSON W B, DILLAMORE I L, BATE P. Contribution of shear banding to origin of Goss texture in silicon iron [J]. Metal Science, 1984, 18(2): 57−66.
[32] SADEGHI F, ZARGAR T, KIM J W, HEO Y U, LEE J S, YIM C H. Role of the annealing twin boundary on the athermal α'-martensite formation in a 304 austenitic stainless steel [J]. Materialia, 2021, 20: 101218.
[33] SONG H Y, LIU H T, JONAS J J, WANG G D. Effect of primary recrystallization microstructure on abnormal growth of Goss grains in a twin-roll cast grain-oriented electrical steel [J]. Materials Design, 2017, 131: 167−176.
[34] PARK J T, SZPUNAR J A. Evolution of recrystallization texture in nonoriented electrical steels [J]. Acta Materialia, 2003, 51(11): 3037−3051.
[35] BARNETT M R, JONAS J J. Influence of ferrite rolling temperature on microstructure and texture in deformed low C and IF steels [J]. ISIJ International, 1997, 37(7): 697−705.
[36] KESTENS L, JONAS J J. Modelling texture change during the static recrystallization of a cold rolled and annealed ultralow carbon steel previously warm rolled in the ferrite region [J]. ISIJ International, 1997, 37(8): 807−814.
[37] HANSEN N. Hall−Petch relation and boundary strengthening [J]. Scripta Materialia, 2004, 51(8): 801−806.
[38] DUNSTAN D J, BUSHBY A J. Grain size dependence of the strength of metals: The Hall−Petch effect does not scale as the inverse square root of grain size [J]. International Journal of Plasticity, 2014, 53: 56−65.

不同热处理温度下薄壁纯铜管的 Goss 织构演变规律

王松伟[1]，宋鸿武[1]，陈 岩[1]，余 琪[1,2]，张士宏[1]

1. 中国科学院 金属研究所 师昌绪先进材料创新中心，沈阳 110016；
2. 江西铜业集团有限公司，南昌 330096

摘 要：采用电子背散射衍射(EBSD)及拉伸试验等方法研究薄壁铜管在热处理过程中显微组织、织构及力学性能的演变规律。结果表明：初始拉拔态铜管组织中以 Copper 和 Y 型织构为主，随着温度升高逐渐转变为强烈的 Goss 型织构。通过高分辨显微组织表征手段可以发现，具有 Goss 取向的再结晶晶粒分别以不同的机制在 Copper 取向和 Y 取向变形晶粒中形核和长大。随着温度的升高，薄壁铜管的抗拉强度逐渐降低，而伸长率受晶粒尺寸和织构组分的共同作用呈先升高后急剧降低的变化趋势。

关键词：薄壁铜管；再结晶行为；Goss 织构；形核机制；退火孪晶

(Edited by Wei-ping CHEN)